Research

Assessment of Extracellular Particles from *Chlorellae sorokin-iana* Culture and Suspension of Washed Erythrocytes Concentrated by Ultrafiltration

Istileulova Yelena[1], Romolo Anna[1], Hočevar Matej[2], Dolinar Jan[3], Jampani Venkata SR[4], Kralj-Iglič Veronika[1,*]

1. University of Ljubljana, Faculty of Health Sciences, Laboratory of Clinical Biophysics, Ljubljana, Slovenia
2. Institute of Metals and Technology, Ljubljana, Slovenia
3. University of Ljubljana, Faculty of Mathematics and Physics, Ljubljana, Slovenia
4. Jozef Stefan Institute, Condensed Matter Physics, Ljubljana, Slovenia

* Correspondence: Veronika Kralj-Iglič; veronika.kralj-iglic@zf.uni-lj.si

Citation: Istileulova Y, Romolo A, Hočevar M, Dolinar J, Jampani VSR, Kralj-Iglič V. Assessment of Extracellular Particles from *Chlorellae sorokin-iana* Culture and Suspension of Washed Erythrocytes Concentrated by Ultrafiltration. Proceedings of Socratic Lectures. **2026**, 14, 85-93. https://doi.org/10.55295/PSL.14.2026.III8

Publisher's Note: UL ZF stays neutral with regard to jurisdictional claims in published maps and institutional affiliations.

Abstract:

Extracellular particles (EPs) are sub-micron sized particles found in biological samples containing cells. While the International Society for Extracellular Vesicles (ISEV) recommends assessment with different orthogonal methods, the technologically advanced golden standard methods for harvesting and assessment are sought. Here we report of harvesting and assessment of EPs from two types of samples: suspension of aged, washed erythrocytes and *Chlorellae sorokiniana* culture. EPs were harvested by reverse ultrafiltration and assessed by Scanning Electron Microscopy (SEM), Interferometric Electron Microscopy (ILM) and UV-vis spectroscopy. We assessed pellets and supernatants of the erythrocyte and microalgae samples (PE, SE, PA, SA, respectively). Average number density of 40 x diluted EPs in PE was (1.16±0.09) $\pm 10^9$/mL and number density of non-diluted EPs in PA was (0.44±0.02) $\pm 10^9$/mL. Average hydrodynamic diameter in SE was (174±72) nm, and in PA it was (252±7) nm. The supernatants did not present notable amount of EPs. Absorption at 260 nm/280 nm in 4 x diluted SE was (3.68±0.04)/(2.64±0.04) arbitrary units (a.u.), in 40 x diluted PE it was (22±0.2)/(25±0.0) a.u., in undiluted PA it was (0.31±0.11)/(0.29±0.13) a.u. and in undiluted SA it was (0.03±0.06)/(0.04±0.01) a.u.. Algae samples contained singular lumps of self-assembly but were poor with proteins and nucleic acids. We conclude that the processing essentially determines the identity of the sample which implies that in order to reach repeatability, the methods should be minimally aggressive to the material, should be made on the same sample and should for this purpose use a minute amount of the sample to enable assessment with other methods. The methods used in this work composed such experimental pipeline that enabled assessment of the samples of in vitro aged erythrocyte EPs and EPs from microalgae culture within hours.

Keywords: Extracellular vesicles; Microalgae; Nanoalgosomes; Erythrocyte microvesicles; Coacervates; Self-asseembly

1. Introduction

EPs are a subject of increasing interest as they are considered mediators of intercellular communication and therefore vectors of vital processes in living organisms (Yanez Mo et al., 2015; Adamo et al., 2021; Welsh et al., 2024; Suresh et al., 2025; Shank et al., 2026; Liangsupree et al., 2026). There is great interest in using EPs in various scientific fields, and medical and industrial applications. The transition of extracellular particles (EPs) from laboratory discoveries to clinical and industrial applications is heavily bottlenecked by current isolation and characterization technologies (Welsh et al., 2024). Current harvesting methods struggle to produce a considerable volume of the sample, and separate EPs with required properties from similar-sized particles. Common contaminants include lipoproteins, protein aggregates, and cellular debris, which can skew downstream analysis. Furthermore, some conventional harvesting techniques suffer from significant EPs' loss. This low recovery rate is particularly problematic for scarce or precious clinical samples like patient plasma or rare cell cultures. Protocols lack uniform automation, leading to high batch-to-batch variability. Results often vary drastically based on the operator, equipment settings, and specific sample handling conditions. High-force isolation techniques, such as standard ultracentrifugation, exert intense shear stress on the sample. This stress can deform, rupture, or induce artificial aggregation of the delicate lipid membranes of EPs. Many laboratory methods require expensive instrumentation and long processing times, and such labor-intensive workflows are entirely unsuited for high-throughput clinical diagnostics or large-scale industrial manufacturing. Therefore, the quest for a "golden standard" method is taking place.

Ultrafiltration (UF) is a membrane-based separation technique widely used to concentrate EPs. It relies on semi-permeable membranes with specific molecular weight cut-offs (MWCO) or pore sizes to retain EPs while allowing smaller molecules and liquid to pass through. Traditional spin filters force the liquid downward through the membrane, smashing the EPs directly into the filter pores. The EV-Spinner operates using a reverse ultrafiltration design, where the liquid is driven through the membrane in the opposite direction of the centrifugal force to reduce membrane clogging (fouling) and severe particle trapping. For microalgae samples, which are naturally prone to clustering and high debris, such design prevents the filter from locking up mid-spin. The polyethersulfone (PES) membrane is chemically treated to be low protein-binding.

In this work we report of using reverse ultrafiltration with EV-Spinner on samples from suspension of aged, washed erythrocytes and the culture of microalgae *Chlorellae sorokiniana*.

2. Material and Methods

2.1. Culturing of microalgae

The microalgae *Chlorella sorokiniana* (strain CCAP 211/8K) were a kind gift from Jelena Danilović Luković from University of Belgrade. They were sourced from the Culture Collection of Algae and Protozoa, UK. They were grown in deionized distilled water with addition of Bold Basal Medium (PhytoTech Labs, Lenexa, Kansas City, USA). The composition of the BBM was: Boric Acid (11.42 mg/L), Manganese Chloride×4H2O (1.44 mg/L), Calcium Chloride Anhydrous (18.87 mg/L), Potassium Hydroxide (31.00 mg/L), Cobalt Nitrate×6H2O (0.49 mg/L), Potassium Phosphate Dibasic (75.00 mg/L), Cupric Sulfate×5H2O (1.57 mg/L), Potassium Phosphate Monobasic (175.00 mg/L), EDTA Disodium Salt (63.61 mg/L), Sodium Chloride (25.00 mg/L), Ferrous Sulfate×7H2O (4.98 mg/L), Sodium Molybdate (1.19 mg/L), Magnesium Sulfate Anhydrous (36.63 mg/L), Sodium Nitrate (250.00 mg/L), Zinc Sulfate×7H2O (8.82 mg/L). Microalgae grew in a 50 mL falcon tube in a shelf of the laboratory having sunlight and conditioned air at 18 °C. We observed no bacteriae under optical microscope in the culture.

2.2. Blood sampling

Blood was donated by an author (a female with no record of disease). Collection was established in the morning after fasting for a minimum of 12 h overnight. A G21 needle (Microlance, Becton Dickinson, Franklin Lakes, NJ, USA) and 2.7 mL evacuated tube with

trisodium citrate (BD Vacutainers, 367714A, Becton Dickinson, Franklin Lakes, NJ, USA) were used.

2.3. Preparation of erythrocyte suspension

To sediment the erythrocytes, blood was centrifuged for 10 min at 300 × g and 18 °C (centrifuge Centric 400/R, Domel, Železniki, Slovenia with swinging rotor). The supernatant (plasma) was haemolytic (**Figure 1**). We removed the plasma from above the buffy coat. The erythrocytes were resuspended in PBS by turning the eprouvette upside-down and centrifuged for 10 min at 300 × g and 18 °C (centrifuge Centric 400/R, Domel, Železniki, Slovenia, with swinging rotor). The supernatant was removed and replaced with PBS. Erythrocytes were resuspended by turning the eprouvette upside-down and centrifuged for 30 min at 500 × g and 18 °C (centrifuge Centric 400/R, Domel, Železniki, Slovenia). The procedure was repeated to yield transparent supernatant above the erythrocytes. The washed erythrocytes suspended in PBS were stored at 4 °C for 15 days.

Figure 1. Blood sample after centrifugation for 10 min at 300 × g and 18 °C showing haemolytic plasma.

2.4. Ultrafiltration of samples

Extracellular particles (EPs) were harvested from 1 mL samples of either suspension of aged washed human erythrocytes or *Chlorella sorokiniana* culture using reverse-flow ultrafiltration. Briefly, individual 1 mL aliquots were loaded directly into EV-Spinner ultrafiltration concentrators (HansaBioMed, Tallinn, Estonia; 100 kDa molecular weight cut-off [MWCO]). The loaded filter units were placed in a centrifuge Centric 400R (Domel d.o.o.) with swinging rotor. The samples were centrifuged at 18 °C and 2500 × g for 15 minutes to drive the liquid and low-molecular-weight elements through the low-protein-binding polyethersulfone (PES) membrane. This step effectively concentrated the retained EPs into a liquid boundary concentrate layer within the retentate chamber, yielding the final pellets (designated PE for the microalgae culture and PA for the erythrocyte suspension). The volume of the retrieved PE was cca 100 µL and of the PA it was cca 50 µL. The corresponding ultrafiltration supernatants (SE for microalgae and SA for erythrocytes) were collected from the filtrate compartment. Both the harvested pellets and collected supernatants were assessed immediately after harvesting, with Interferometric Light Microscopy (ILM), and UV-vis spectroscopy.

2.5. Electron microscopy

Scanning Electron Microscopy (SEM). A drop of 5 µL of sample was loaded onto aluminum stands covered with thin layer of polymers based on cyanoacrylates (Jampani et al., 2024) and let to dry in air. The sample was examined with a Thermo Fisher Scientific Apreo 2 microscope with EDS/EBSD detector, low vacuum mode.

2.6. Assessment of density and viscosity

We measured the density of the supernatants. There was not enough volume of the pellets (required 1mL) available for the measurement with the above described instrument, so we used the supernatant density as an estimate also for pellets. The density was then used as an input to assess viscosity, and viscosity was used as an input to assess hydrodynamic diameter of nanoparticles by ILM. Density measurement was performed using an oscillating U-tube Density Meter (DMA 1002, Anton Paar, Graz, Austria). 1 mL sample was placed in the measuring cell, which was subjected to acoustic oscillations. Dynamic viscosity was measured using a falling ball micro viscometer (Lovis 2000 M, Anton Paar, Graz, Austria with Lovis 1.59 Short Capillary). Temperature and measurement angle were set at 20°C and 45° respectively.

2.7. Interferometric Light Microscopy (ILM)

EP samples were measured with ILM using Videodrop (Myriade, Paris, France)(Boccara et al., 2016; Romolo et al., 2022; Korenjak et al., 2024). Samples were diluted to enable optimal performance of the instrument (in the range of (0.5 to 5)×10^9/mL). 7 µl of sample was placed between cover glasses and illuminated by a 2 W blue LED light. Threshold value was 4.2. The average concentration (ILMc) and D_h of EPs were determined for each sample. The position of a particle was captured in the recorded video (movie). We set a limit of 20 movies or 300 detected EPs to assess the EPs in the sample. We used the software QVIR 2.6.0 (Myriade, Paris, France) to process the images (movies). D_h was determined by the Einstein-Stokes equation using the measured data of viscosity and density obtained as described above.

2.8. UV - vis spectroscopy

Three microliters droplets of samples were placed on the stand of a Nanodrop UV spectrometer (Thermofischer Scientific, Waltham, MA, USA) and assessed for ultraviolet-visible spectrum (UV-Vis) absorbance. The wavelengths 260 nm and 280 nm were considered in all samples, while the wavelength 430 nm was considered in erythrocyte samples, and wavelengths 460 nm and 690 nm were considered in microalgae samples. Samples were mixed before measurement.

2.9. Statistical Analysis

All data were analysed using descriptive statistics. All measurements were performed in triplicate and are presented as an average and standard deviation.

3. Results

Pellets of ultrafiltration (PE and PA) indicated the presence of EPs in samples while supernatants of ultrafiltration (SE and SA) were practically devoid of EPs (**Table 1**); in supernatants, the number densities of EPs were under the operational detection limits of the ILM (**Table 1**).

Table 1. Number density of EPs *n*, hydrodynamic diameter D_h and absorbances (A) at respective UV and visual light wavelengths for pellets and supernatants of the ultrafiltration. PE: ultrafiltration pellet from in vitro aged washed erythrocyte suspension, SE: ultrafiltration supernatant from in vitro aged washed erythrocyte suspension, PA: ultrafiltration pellet from microalgae culture, SA: ultrafiltration supernatant from microalgae culture. The results are given by the averages of three measurements ± standard deviations.

Variable	Dilution	n ×10^9/mL	D_h (nm)	A260	A280	A430	A460	A690
PE	40	1.16±0.09	168±6	22.3±0.23	24.8±0.0	73.6±0.70	/	/
SE	4	0.01±0.00	174±72	3.68±0.04	2.64±0.04	6.63±0.06	/	/
PA	1	0.44±0.02	252±7	0.31±0.11	0.29±0.13	/	0.04±0.04	0.04±0.04
SA	1	0	0	0.03±0.06	0.04±0.01	/	0	0

Imaging the pellet PE, **Figure 2A** shows extensive dendritic crystalline structures, which are classic signatures of dried buffer salts (like PBS) or crystallized proteins (such as hemoglobin). Panel **B** highlights distinct, spherical nano-sized particles (erythrocyte EPs) embedded within dense matrix. Imaging the supernatant SE, **Figure** 2**C** reveals scattered, cuboidal/geometric crystal lattices, typical of clean salt precipitation from a dried buffer solution. Panel **D** appears largely smooth and featureless, displaying an empty background devoid of the characteristic globular clusters seen in the pellet. Panels **E, F** (Fixed/Stained SEM Control) and **G** (cryogenic transmission electron microscope image)(Božič et al., 2021; Jozelj et al., 2022) are shown for comparison. A notable amount of EPs survived the treatment by 80 °C. The protein and nucleic acid content in the erythrocyte samples was considerable, in particular the clearly expressed peak pertaining to haemoglobin. The values of the absorbance at 430 nm in the ultrafiltration pellet were the highest detected among the samples. The pellet from microalgae PA presented a detectable amount of EPs but did not define a peak at the chlorophyll absorbance wavelengths 460 nm and 690 nm.

C (Panel **E**). The cryo-transmission electron micrograph (**Figure 2G**) reveals intact, well-defined, oval-to-elongated vesicular membranes filled with dense internal contents, confirming the presence of true biogenic lipid-bilayer extracellular vesicles.

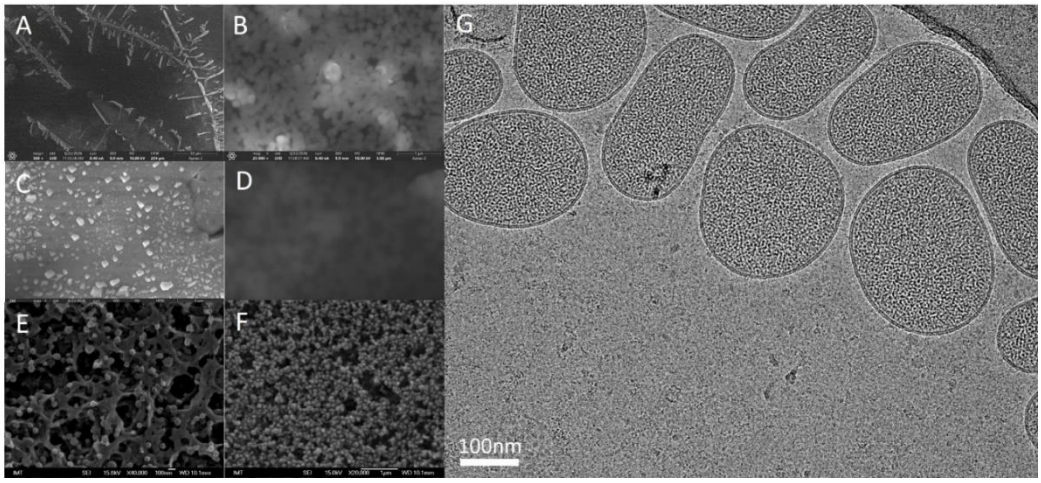

Figure 2. Scanning electron microscopy (SEM) and cryogenic transmission electron microscopy (cryo-TEM) images of erythrocyte-derived fractions. (A, B) SEM micrographs of the raw ultrafiltration pellet containing erythrocyte extracellular particles (EPs) embedded in crystalline matrix. (C, D) SEM micrographs of the corresponding raw ultrafiltration supernatant, displaying clean buffer salt precipitation and an absence of vesicular clusters. (E) SEM micrograph of fixed, stained, and heavy-metal-sputtered erythrocyte EPs following thermal treatment at 80 °C. (F) SEM micrograph of control fixed, stained, and heavy-metal-sputtered erythrocyte EPs. (G) Cryo-TEM micrograph demonstrating intact, well-defined biogenic erythrocyte extracellular vesicles (EVs). Panels E–G are reproduced from Božič et al., 2021 (available under a Creative Commons Attribution 4.0 International License [CC BY 4.0]).

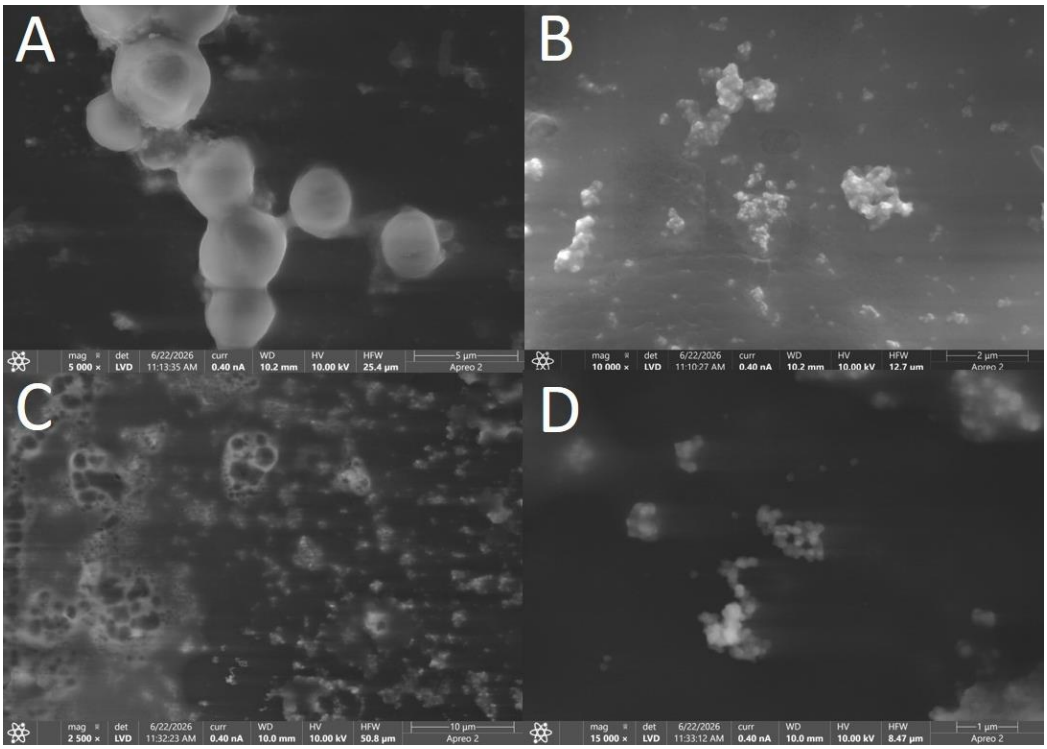

Figure 3. Scanning electron microscopy (SEM) micrographs of raw ultrafiltration pellet fractions (PA) from a *Chlorellae sorokiniana* microalgae culture. (A) Low-magnification overview showing distinct, spherical microalgae cells tightly associated with clusters of sub-micron globular extracellular particles (EPs). (B–D) Intermediate and high-magnification views of alternate fields revealing a repeating, porous extracellular polymeric substance network and self-assembled organic film embedded with clustered, nano-sized structures.

Imaging the pellet PA, **Figure 3A** shows distinct, spherical microalgae cells (~3–5 μm in diameter) tightly associated with clusters of much smaller, globular extracellular particles (EPs). **Figures 3B-D** reveal a repeating, porous network structure resembling a dried liquid film or a polymer surface with embedded clustered nano-sized globular particles. Microalgae cultures often contain complex extracellular polymeric substances, sticky polysaccharides, and rigid cell walls that can build up globular nano and microstructures.

The protein and nucleic acid content in the erythrocyte samples was considerable, in particular the clearly expressed peak pertaining to haemoglobin. The values of the absorbance at 430 nm in the ultrafiltration pellet were the highest detected among the samples. The pellet from microalgae PA presented a detectable amount of EPs but did not define a peak at the chlorophyll absorbance wavelengths 460 nm and 690 nm.

4. Discussion

4.1. Thermodynamic dispersity and dilution-induced colloidal aggregation

Morphological analysis via scanning electron microscopy (SEM) revealed distinct lumped nanoparticles within the *Chlorella sorokiniana* microalgae fractions. In highly dilute solutions, dispersed individual particles operate in a state of thermodynamic instability due to their high free energy. To minimize the free energy, adjacent particles drift into a coordination sphere, co-localizing into cohesive clusters or "particle swarms" (**Figures 3B–D**). This phenomenon is accelerated during sample preparation. As a droplet desorbs and dries upon the SEM stub covered with nanoscale polymer films (Jampani et al., 2024), the receding capillary meniscus acts as a physical net. The fluid front drives individual scattered particles and pre-existing particulate swarms into closer proximity, ultimately locking them into highly visible, clumped networks. Consequently, the micro-structures observed within the microalgae supernatants (SA) are best characterized as dilution-induced colloidal aggregates or flocculated particle swarms.

4.2. Biopolymer condensation paradox: microalgae mucilage vs. erythrocyte hemoproteins

The self-assembly behavior in microalgae samples is driven by the unique biochemistry of phycological secretomes. Unicellular green algae are notorious for secreting vast quantities of extracellular polymeric substances, commonly referred to as mucilage. This complex extracellular matrix consists primarily of high-molecular-weight heteropolysaccharides, glycoproteins, and proteoglycans. Within the raw culture media, the mucilage exists in a highly dynamic equilibrium between fully dissolved single polymer chains and larger assembled gel networks. During pressure-driven reverse ultrafiltration, unassembled polysaccharide chains or low-molecular-weight glycoprotein subunits align linearly under convective flow, easily slipping through the 3–10 nm pore channels of a 100 kDa membrane. Upon entering the filtrate chamber, the localized shear forces from fluid processing combined with subsequent concentration-driven cross-linking trigger these amphiphilic biopolymers to spontaneously condense into globular nano-aggregates. Importantly, pseudo-EP structures lack an authentic phospholipid bilayer. They represent highly dynamic, transient gel matrices capable of shifting morphology under localized environmental conditions. Such behavior highlights a critical, source-specific artifact unique to microalgal harvesting workflows that must be carefully distinguished from biogenic, bilayer-enclosed extracellular vesicles (EVs). In contrast, washed erythrocyte suspensions do not secrete sticky, highly cross-linking plant polysaccharides. The background of mammalian red blood cell streams is instead dominated by structurally stable proteins, specifically hemoglobin. If individual 64 kDa hemoglobin tetramers pass through the ultrafiltration barrier, they remain stable monodisperse units in solution or form standard geometric crystalline precipitates upon drying (**Figures 2A and 2C**) rather than self-assembling into biomimetic nano-spheres.

4.3. Historical nomenclature and the biophysical context of ultrafiltration

The isolation and characterization of submicron extracellular structures—historically labeled as microparticles, exosomes, paramural bodies, or exocellular fragments, and modernly consolidated under the umbrella of extracellular vesicles (EVs) and extracellular particles (EPs) — has long presented a biophysical challenge. Foundational researchers in the 1970s and 1980s recognized that there are different methods to resolve membranous nanoparticles from complex macro-solute matrices. Early pioneers successfully integrated ultrafiltration to concentrate and purify submicron vesicles (Blatt et al., 1970; Porter, 1972;

Cotton et al., 1975; Tutunijan, 1982; Cheryan, 1986). Also, mammalian body fluids were considered as sources of EPs (Lutz et al., 1977; Panakov et al., 1977; Stagmayer et al., 1982; Greenwalt et al., 1984; Wiggins et al., 1986; Johnstone et al. 1987). Johnstone et al. coined the term "exosome" in describing how maturing sheep reticulocytes clear unwanted proteins (like the transferrin receptor) via the fusion of multivesicular bodies with the plasma membrane (Johnstone et al., 1987).

When extracting extracellular fractions from unicellular green algae or plants, early investigators were forced to confront thick, carbohydrate-rich matrices and dense wall components. To isolate EPs without inducing mechanical cell lysis, researchers implemented sequential filtration and pressure-driven membrane concentration systems to successfully harvest exocellular particles (Halperin et al., 1967; McLean et al., 1972; Marchant et al., 1986; Atkinson et al., 1972; Grov et al., 1981, Vreeland et al., 1984). It was identified that the harvesting of the particles was severely hampered by the co-purification by the mucilage (Atkinson et al., 1972).

Our current pipeline directly addresses these historical limits by utilizing reverse ultrafiltration to harvest EPs from both washed erythrocytes and *Chlorellae sorokiniana* cultures. In membrane separation physics, dead-end filtration configurations suffer from rapid concentration polarization and gel-layer cake formation (Blatt et al., 1970; Porter, 1972), wherein accumulated macro-solutes blind the membrane pores and trap smaller vesicles. By implementing a reverse ultrafiltration strategy, we successfully mitigated this cake formation.This processing efficiency is directly reflected in our characterization data. The high concentration of EPs captured in the erythrocyte pellet (PE: $(1.16 \pm 0.09) \times 10^9$ /mL) at 40 × dilution) versus the microalgae pellet (PA: $(0.44 \pm 0.02) \times 10^9$ /mL), non-diluted) demonstrates that reverse ultrafiltration functions effectively across radically different biological matrices.

Crucially, our supernatants (SE and SA) presented no notable amounts of EPs, confirming that the molecular cutoff of the filter membrane efficiently retained the target particles without letting them slip through or shear into smaller fragments—a common issue when using early, non-optimized membrane configurations.

4.3. Spectroscopic fingerprints and the dilution-identity law

Our UV-vis spectroscopy data reveals a striking contrast between the two sources that can be explained through historical biochemical frameworks. The 40-fold diluted erythrocyte pellet (PE) showed high absorption at 260/280 nm ((22 ± 0.2 a.u.) / (25 ± 0.0 a.u.))(**Table 1**), pointing to a dense corona of proteins and hemoglobin remnants typical of aged, ATP-depleted erythrocytes. Conversely, the *Chlorellae sorokiniana* pellet (PA) was remarkably poor in proteins and nucleic acids ((0.31 ± 0.11) a.u. / (0.29 ± 0.13 a.u.))(**Table 1**). Low protein/nucleic acid profile in algae agrees with previous results that *Chlorella sorokiniana* cell-wall-associated fractions are primarily composed of structural lipids and non-proteinaceous polymers, rather than soluble cytoplasmic proteins (Grov and Taylor, 1981). The singular lumps of self-assembly seen in our algae samples likely represent the structural arrangement of these exocellular matrices as they interact with trace ambient polysaccharides, a behavior predicted by Vreeland and Laetsch (1984). Structurally identical, micro-sized globular lumps are present in both the ultrafiltration pellet (PA; **Figures 3A and 3B**) and the ultrafiltration supernatant (SA; **Figures 3C and 3D**). The primary differentiation between the two fractions is quantitative, with a lower density of these micro-structures observed in the supernatant. Rather than indicating a failure of the ultrafiltration membrane retention, this phenomenon points to a continuous, post-filtration spontaneous thermodynamic self-assembly of mucilage and sticky polysaccharides. Free macromolecules passing through the membrane pores into the supernatant fluid continuously aggregate to reach an operational energy minimum, organizing into macro-molecular clusters in situ after the filtration process is complete.

Because of this highly dynamic behavior, we have explicitly reported the number densities of the EPs at their exact measured dilutions (**Table 1**). Due to the fragile colloidal nature of EPs, subjecting these samples to additional or un-optimized dilution steps alters their thermodynamic equilibrium. Such shifts are likely to drive individual particles into entirely different structural states, shifting the identity, composition, size, and shape of the observed clusters. Therefore, to ensure reproducible characterization, processing pipelines must consume minute sample volumes and avoid aggressive post-isolation modifications.

The high concentration of EPs captured in the erythrocyte pellet ($1.16 \pm 0.09 \times 10^9$ /mL) versus the microalgae pellet ($0.44 \pm 0.02 \times 10^9$ /mL) (**Table 1**) demonstrates that reverse ultrafiltration functions effectively across radically different biological matrices. Crucially, our supernatants (SE and SA) presented no notable amounts of EPs, confirming that the molecular cutoff of our membranes efficiently retained the target particles without letting them slip through or shear into smaller fragments—a common issue when using early, non-optimized membrane configurations (Cheryan, 1986).

The post-filtration assembly clarifies the discrepancy observed with our ILM measurements, which recorded no particles for the SA fraction (**Table 1**). Because these self-assembled organic lumps rapidly exceed the sub-micron scale, they transcend the operational detection ceiling of standard ILM tracking (approximately 800 nm). Crucially, however, the optical background of the SA was notably clearer than that of the PA (**Figure 3**).

5. Conclusions

By implementing a reverse ultrafiltration processing pipeline paired with non-destructive, minute-volume orthogonal characterization methods (SEM, ILM, and UV-vis spectroscopy), we established a rapid experimental workflow capable of assessing EPs in samples within a matter of hours. The qualitative and quantitative results from the included analytical methods demonstrated excellent agreement across both biological matrices. The mammalian erythrocyte pellet (PE) was highly enriched with both EPs and co-isolated proteins and nucleic acids, exhibiting distinct globular morphologies of EPs consistent with membrane-enclosed vesicles. Conversely, the microalgae pellet (PA) was comparatively poor in native EPs, proteins, and nucleic acids. In both post-filtration supernatants (SE and SA), sub-micron EPs were thoroughly depleted, falling beneath the operational detection limits of the ILM tracking system. However, while the erythrocyte supernatant (SE) retained a high background of stable soluble hemoproteins and nucleic acids, the microalgae supernatant (SA) was largely devoid of macromolecular signatures. Morphologically, the micro-lumps observed in the algal supernatant (SA) lacked the distinct smooth geometry characteristic of membrane-enclosed biogenic vesicles. Instead, they represent dynamic, dilution-induced colloidal matrices that undergo spontaneous thermodynamic self-assembly from cell wall polysaccharides and mucilage subunits after passing through the filtration membrane. Ultimately, this work demonstrates that reverse ultrafiltration provides a highly efficient, gentle, but low-volume mechanism to concentrate and harvest native EPs from radically different cellular sources.

Funding: This research was supported by European Union's Horizon 2020 research and innovation program FarmEVs under grant agreement No 109338, and by Slovenian Research and Innovation Agency ARIS P2-0132, P3-0388, J2-60051, J3-60063, and N1-0400.

Conflicts of Interest: The authors declare no conflict of interest.

References

1. Adamo G, Fierli D, Romancino DP, Picciotto S, Barone ME, Aranyos A, Božič D, Morsbach S, Raccosta S, Stanly C, et al. Nanoalgosomes: Introducing extracellular vesicles produced by microalgae. J Extracell Vesicles. 2021; 10:e12081. DOI:10.1002/jev2.12081
2. Atkinson AW Jr, Gunning BES, John PCL. Sporopollenin in the cell wall of Chlorella and other algae: ultrastructure, chemistry, and incorporation of ^{14}C-acetate, studied in synchronous cultures. Planta. 1972; 107:1-32. DOI: 10.1007/BF00386053
3. Blatt WF, Dravid A, Michaels AS, Nelsen L. Solute polarization and cake formation in membrane ultrafiltration: causes, consequences, and control. In Membrane Science and Technology, JE Flinn ed. Plenum Press, New York 1970:47-97.
4. Boccara M, Fedala Y, Bryan CV, Bailly-Bechet M, Bowler C, Boccara AC. Full-field interferometry for counting and differentiating aquatic biotic nanoparticles: from laboratory to *Tara* Oceans. Biomed Opt Express. 2016; 7:3736-3746. DOI: 10.1364/BOE.7.003736
5. Božič D, Hočevar M, Kisovec M, et al. Stability of Erythrocyte-Derived Nanovesicles Assessed by Light Scattering and Electron Microscopy. Int J Mol Sci. 2021; 22:12772. DOI:10.3390/ijms222312772
6. Cheryan M. Ultrafiltration Handbook. Technomic Publishing Company; 1986.
7. Colton CK, Friedman S, Wilson DE, Martin JS. Ultrafiltration of large molecules through asymmetric membranes. J Clin Invest. 1975; 55:511-525. DOI:10.1172/JCI107957

8. Greenwalt TJ, Bryan DJ, Dumas W. Erythrocyte membrane vesiculation in vivo and in vitro. Br J Haematol. 1984; 58:241-253. DOI: 10.1111/j.1365-2141.1984.tb06082.x
9. Grov A, Taylor FJ. The isolation of cell wall-associated membrane fractions from Chlorella sorokiniana. J Gen Microbiol. 1981; 124:215-224. DOI:10.1099/00221287-124-2-215
10. Halperin W, Jensen WA. Ultrastructural changes during growth and embryogenesis in carrot cell cultures. J Ultrastruct Res. 1967; 18:428-443. DOI: 10.1016/S0022-5320(67)80130-9
11. Jampani VSR, Škarabot M, Mur U, Baigl D, Jonas U, Lagerwall JPF, Ravnik M, Anyfantakis M. Water-Templated Growth of Interfacial Superglue Polymers for Tunable Thin Films and In Situ Fluid Encapsulation. Adv Mater. 2024; 36(40):e2408243. DOI: 10.1002/adma.202408243
12. Johnstone RM, Adam M, Hammond JR, Orr L, Turbide C. Vesicle formation during reticulocyte maturation. Association of transferrin receptor with the shedding vesicles (exosomes). J Biol Chem. 1987; 262:9412-9420. DOI: 10.1016/S0021-9258(18)47533-X
13. Jozelj M, Košir T, Božič D, Hočevar M, Pajnič M, Iglič A, Jeran M, Kralj-Iglič V. Morphological parameters of erythrocyte extracellular vesicles at hypoosmotic and isoosmotic conditions. Proc Socrat Lect. 2022; 7:111–115. DOI: 10.55295/PSL.2022.D16
14. Korenjak B, Tratenšek A, Arko M, Romolo A, Hočevar M, et al. Assessment of Extracellular Particles Directly in Diluted Plasma and Blood by Interferometric Light Microscopy. A Study of 613 Human and 163 Canine Samples. Cells. 2024; 13:2054. DOI: 10.3390/cells13242054
15. Liangsupree T, Multia E, Riekkola ML. Recent advances in modern extracellular vesicle isolation and separation techniques. J Chromatogr A. 2026; 1767:466602. DOI:10.1016/j.chroma.2025.466602
16. Lutz HU, Liu SC, Palek J. Release of spectrin-free vesicles from human erythrocytes during ATP depletion. I. Characterization of spectrin-free vesicles. J Cell Biol. 1977; 73:548-560. DOI:10.1083/jcb.73.3.548
17. Marchant R, Robards AW. Membrane systems associated with the plasmalemma of plant cells. Ann Bot. 1968; 32:457-471. DOI: 10.1093/oxfordjournals.aob.a084226
18. Mclean RJ, Laurence LS. Characteristics of the exocellular particles of Chlorella. Phycologia. 1972; 11:191-197. DOI: 10.2216/i0031-8884-11-2-191.1
19. Porter MC. Concentration polarization in membrane ultrafiltration. Ind Eng Chem Prod Res Dev. 1972; 11:234-248. DOI:10.1021/i360043a002
20. Romolo A, Jan Z, Bedina Zavec A, Kisovec M, Arrigler V, Spasovski V, Podobnik M, Iglič A, Pocsfalvi G, Kogej K, et al. Assessment of Small Cellular Particles from Four Different Natural Sources and Liposomes by Interferometric Light Microscopy. International Journal of Molecular Sciences. 2022; 23:15801. DOI: 10.3390/ijms232415801
21. Schank MB, Zhao J, Wang L, Moorman JP, Yao ZQ. Extracellular Vesicles: A Comprehensive Review of Their Origins, Functions, and Therapeutic Potential. Biomedicines. 2026; 14:495. DOI: 10.3390/biomedicines14030495
22. Stegmayr B, Ronquist G. Promotive effect on human sperm progressive motility by prostasomes. Urol Res. 1982; 10:253-257. DOI:10.1007/BF00255932
23. Suresh PS, Zhang Q. Comprehensive Comparison of Methods for Isolation of Extracellular Vesicles from Human Plasma. J Proteome Res. 2025; 24:2956-2967. DOI: 10.1021/acs.jproteome.5c00149
24. Trams EG, Lauter CJ, Salem N Jr, Heine U. Exfoliation of membrane ecto-enzymes in the form of microvesicles. Biochim Biophys Acta. 1981; 645:63-70. DOI: 10.1016/0005-2736(81)90512-5
25. Tutunjian RS. Ultrafiltration processes in biotechnology. Ann N Y Acad Sci. 1983; 413:238-253. DOI:10.1111/j.1749-6632.1983.tb47897.x
26. Vreeland V, Slomich M, Laetsch WM. Monoclonal antibodies as molecular probes for cell wall antigens of the brown alga, Fucus . Planta. 1984; 162:506–517. DOI:10.1007/BF00399916
27. Welsh JA, Goberdhan DCI, O'Driscoll L, Buzas EI, Blenkiron C, Bussolati B, Cai H, Di Vizio D, Driedonks TAP, Erdbrügger U et al. Minimal information for studies of extracellular vesicles (MISEV2023): From basic to advanced approaches. J Extracell Ves. 2024; 13:e12404. DOI: 10.1002/jev2.12404
28. Wiggins RC, Glatfelter A, Kshirsagar B, Niles S. Submicron membrane-bound particles (vesicles) in normal urine. Nephron. 1986; 43:224-228. DOI: 10.1159/000183842
29. Yáñez-Mó M, Siljander PR, Andreu Z, Bedina Zavec A, Borràs FE, Buzas EI, Buzas K, Casal E, Cappello F, Carvalho J, et al. Biological properties of extracellular vesicles and their physiological functions. J Extracell Vesicles 2015; 4: 27066. DOI:10.3402/jev.v4.27066